



OPEN

SUBJECT AREAS:

SENSORS

BIOANALYTICAL CHEMISTRY

BIOSURFACES

ELECTROCHEMISTRY

Capturing intercellular sugar-mediated ligand-receptor recognitions via a simple yet highly biospecific interfacial system

Zhen Li¹, Si-Si Deng², Yi Zang², Zhen Gu¹, Xiao-Peng He¹, Guo-Rong Chen¹, Kaixian Chen^{1,2}, Tony D. James^{1,3}, Jia Li² & Yi-Tao Long¹Received
19 March 2013Accepted
11 July 2013Published
29 July 2013

Correspondence and requests for materials should be addressed to X.P.H. (xphe@ecust.edu.cn); J.L. (jli@mail.shcnc.ac.cn) or Y.T.L. (ytlong@ecust.edu.cn)

¹State Key Laboratory of Bioreactor Engineering, and Key Laboratory for Advanced Materials & Institute of Fine Chemicals, East China University of Science and Technology, Shanghai 200237, PR China, ²National Center for Drug Screening, State Key Laboratory of Drug Research, Shanghai Institute of Materia Medica, Shanghai Institutes of Biological Sciences, Chinese Academy of Sciences, Shanghai 201203, PR China, ³Department of Chemistry, University of Bath, Bath, BA2 7AY, UK.

Intercellular ligand-receptor recognitions are crucial natural interactions that initiate a number of biological and pathological events. We present here the simple construction of a unique class of biomimetic interfaces based on a graphene-mediated self-assembly of glycosyl anthraquinones to a screen-printed electrode for the detection of transmembrane glycoprotein receptors expressed on a hepatoma cell line. We show that an electroactive interface confined with densely clustered galactosyl ligands is able to ingeniously recognize the asialoglycoprotein receptors on live Hep-G2 cells employing simple electrochemical techniques. The only facility used is a personal laptop in connection with a cheap and portable electrochemical workstation.

A multitude of life events are modulated by intercellular ligand-receptor recognitions. And it is believed that the interactions between glycans that massively distribute in all living organisms and their specific transmembrane receptors initiate myriad physiological and pathological events such as cell-cell adhesion, cellular differentiation, cell growth and cytokinesis, bacterial infection, viral invasion and cancer metastasis^{1–8}. Consequently, the elucidation of these interactions may contribute to decipherment of the “Glycomics” and facilitate early-state disease diagnosis, and sugar-based drug and vaccine development^{9–12}.

However, the measurement of sugar-protein interactions has been a difficult task because of the low binding affinity between a glycan and its cognate protein. To address this issue, the so-called glycoarray technique has been developed, which is based on the immobilization of neo-glycoconjugates onto a solid surface for detecting fluorescently tagged analytes^{13–17}. Indeed, this elegant method has been of particular interest due to the following merits: (i) a very small amount of sugars are required; (ii) confining sugars on surfaces in a densely clustered manner gives rise to a much enhanced binding avidity with receptors, resulting in signal amplification.

Despite the contribution of this technology towards the progress of the glycomics, however, some flaws remain that hamper its wide-spread utilization. For instance, immobilization of sugar ligands onto solid surfaces requires substantial effort and the bio-specificity of chemically labelled analytes might be compromised. In addition, costly facilities are used for detection, making such a means relatively impractical for the majority of research groups. We present here the unique construction of a simple yet highly biospecific interfacial system based on a one-step graphene-mediated self-assembly of anthraquinonyl glycosides to a screen-printed electrode (SPE) for sensitive detection of intercellular sugar ligand-receptor interactions. We show that the designed system has the ability to exquisitely capture glycoprotein receptors exclusively expressed on live cancer cells employing facile electrochemical methods and economic facilities.

Results

Synthesis. The electroactive glycosyl anthraquinones (GAs) were prepared by a click reaction^{18,19} of azido glucoside (a) and galactoside (b) with, respectively, a bis-(c) and a mono-(d) *O*-propargyl anthraquinone²⁰. Triazolyl glycosyl acetates 1'–4' were afforded with reasonable yields, and a subsequent deacetylation led to the desired dimeric and monomeric GAs 1–4 (Fig. 1 and Scheme S1).

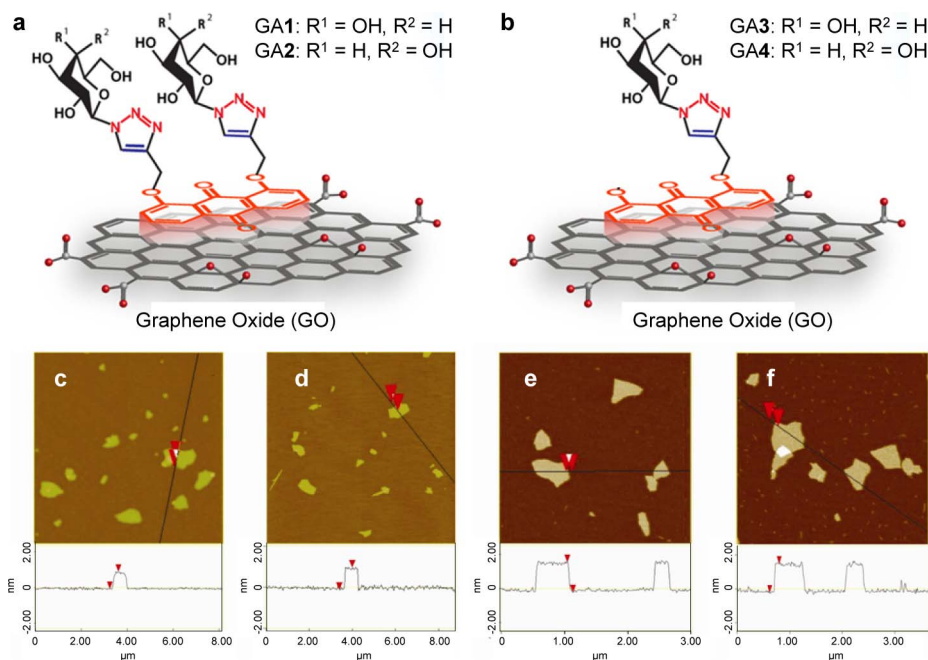


Figure 1 | Schematic representation of graphene oxide (GO)-glycosyl anthraquinones (GAs) and characterization of the stacked composites by atom force microscope (AFM). (a) GA1 and GA2, and (b) GA3 and GA4 stacked to GO. AFM images of (c) GO-GA1, (d) GO-GA2, (e) GO-GA3 and (f) GO-GA4 on mica surface.

Fabrication of the biomimetic interface. Graphene oxide (GO), a low-cost, scalable (vs. other carbonaceous materials such as fullerene and carbon nanotube) yet powerful carbon flake that has fulfilled the fabrication of many ingenious biosensors and devices^{21–28}, was used to facilitate the fixation of the GAs onto SPE. Self-assembly of GAs 1–4 to GO prepared from graphite powder according to the modified Hummers method²⁹ was first realized via π -stacking (Fig. 1a and Fig. 1b). Atom force microscope used to identify the formation of the GO-GAs showed that the height of bare GO is ~ 1.0 nm (Fig. S1a) which agrees with that of exfoliated GO sheets reported previously³⁰. In contrast, the height of all GO-GAs grew to ~ 1.7 nm, indicating the adsorption of the GAs onto GO surface (Fig. 1c to Fig. 1f). Raman and Fourier Transformation Infrared (FTIR) spectroscopic analyses further confirmed the formation of the π -stacked composites. All Raman spectra displayed the characteristic D band and G band of GO at 1354 cm^{-1} and 1604 cm^{-1} , respectively (Fig. S2). The increased I_D/I_G ratio of GO-GAs (Fig. S2a2–Fig. S2a5) compared to that of GO (Fig. S2a1) signifies an increased disorder of carbon sp^2 -hybridization due to the presence of the triazolyl anthraquinone of the former. Adsorption peaks assignable to the methylene and triazole groups of GAs were observed in the FTIR spectra of the GO-GAs (Fig. S2b2–Fig. S2b5).

Production of the SPEs that consist of a graphite-based working electrode was actualized according to our previously described method³⁰. These low-cost electrodes can be produced massively, representing an ideal class of electrochemical micro-device. The interfacial systems were then finalized by simply spotting the GO-GAs ($3\ \mu\text{L}$) to the working electrode of SPE. Cyclic voltammetry (CV) was primarily used to depict the electrochemical processes of the interfacial GO-GAs (Fig. 2) in a phosphate buffered saline (PBS) buffer; an electrode confined with GO-1,8-dihydroxyanthraquinone (AQ-OH) was used as control (Fig. S3a). By increasing the scan rates from 0.02 to 0.12 V/s , the CVs of all redox couples showed a pair of symmetric peaks with a gradually increased peak current. Plotting of the scan rates as a function of the corresponding anodic and cathodic peak currents resulted in linear correlations (insets of Fig. 2a–d and

Fig. S3b), which means that the oxidation and reduction processes of the electroactive species are surface-controlled. This observation suggests that the GO-GAs have been successfully confined on the SPE surfaces.

The cathodic to anodic peak current separation for AQ-OH is 50 mV , whereas those for the GAs 1, 2, 3, and 4 are 100 mV , 96 mV , 74 mV and 56 mV , respectively, indicating that the electron transfer (ET) process of the former is kinetically faster than those of the latter. This could be ascribed to the presence of the triazolyl glycosides on the AQ moiety, impeding the ET. We also observed that the reduction peak potential (-0.58 V) of AQ-OH centered more negatively than those of the GAs 1–4 ($\sim -0.43\text{ V}$), suggesting that the latter can be reduced more easily than the former³¹. The surface coverage concentration for SPE of GAs 1, 2, 3 and 4 were determined to be $4.4 \times 10^{-9}\text{ mol cm}^{-2}$, $5.0 \times 10^{-9}\text{ mol cm}^{-2}$, $3.5 \times 10^{-9}\text{ mol cm}^{-2}$ and $4.2 \times 10^{-9}\text{ mol cm}^{-2}$, respectively. However, addition of GO-free GA1 (Fig. S4a) and GA2 (Fig. S4b) to SPE led to apparently decreased peak currents, suggesting that GO can more compactly cluster the electroactive GAs on the electrode.

Function of the biomimetic interface. With the biomimetic interfaces in hand, their sensing ability was first tested in a Tris-HCl buffer (pH 7.0) containing Ca^{2+} and Mn^{2+} via differential pulse voltammetry (DPV) for lectins, proteins that contain sugar-recognition domains³². Primarily, addition of the mannose/glucose-specific Concanavalin A (Con A, $10\ \mu\text{M}$) and galactose-specific peanut agglutinin (PNA, $10\ \mu\text{M}$) to GO-free SPEs doped with GA1 and GA2, respectively, led to a notable current quenching (by $\sim 60\%$, Fig. S4). However, addition of the lectins reversely also decreased the current intensity (by $\sim 15\%$), suggesting that both the specific sugar-lectin recognitions and non-specific protein adsorptions on the electrode surface might have contributed to the signal decay.

Subsequently, we interrogated the biospecificity of the SPEs confined with the GO-GAs. Incubation of the specific lectin ($8\ \mu\text{M}$) with the corresponding SPE (Con A to the glucose-confined 1 and 3, and PNA to the galactose-confined 2 and 4) led to a clear current

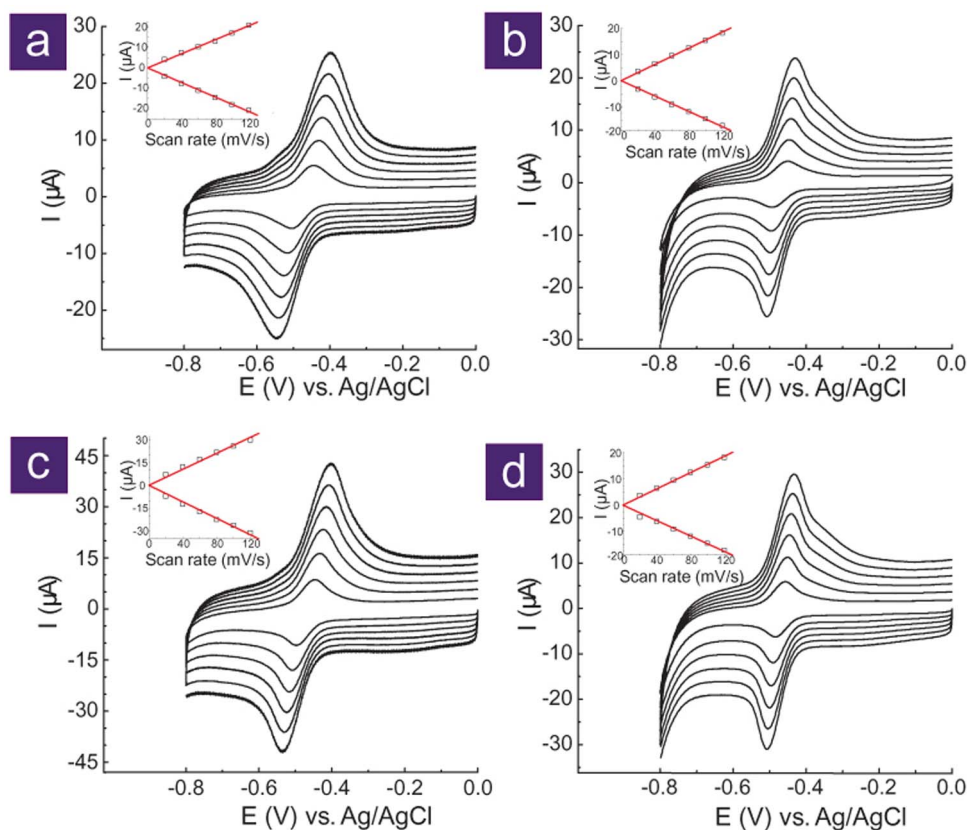


Figure 2 | Cyclic voltammetry (CV) of screen printed electrodes (SPEs) confined with the GO-GAs. CVs of SPEs confined with (a) GO-GA1, (b) GO-GA3, (c) GO-GA2 and (d) GO-GA4 in phosphate buffered saline (PBS, pH 7.0) with different scan rates (Insets: plotting of current, I , as a function of scan rate). All first scans were initiated in the positive direction from -0.8 V.

quenching, whereas the addition of the two lectins reversely did not induce noticeable current change (Fig. 3). Moreover, the presence of a panel of other non-specific lectins ($8 \mu\text{M}$) including the *N*-acetyl-galactosamine-specific soybean agglutinin (SBA), the fucose-specific *Ulex europaeus* agglutinin (UEA-I), the *N*-acetyl-glucosamine-specific wheat germ agglutinin (WGA), and the mannose-specific *Pisum sativum* agglutinin (PSA) caused trivial current alternations of the SPEs confined with GO-GAs 1 and 2 (Fig. 3). We note that, however, the addition of SBA to the galactose-confined SPE 2 led to a minor current quenching; because besides *N*-acetyl-galactosamine, this lectin also binds with its structurally analogous galactose with a lesser affinity. Pre-incubation of free methyl *O*-mannoside with Con A and methyl *O*-galactoside with PNA inhibited the current quenching of 1 and 2, respectively, confirming that the signal is derived from specific sugar-lectin interactions (Fig. S5). These data positively corroborate that the SPEs confined with GO-GAs are bio-specific.

The peak current of the SPEs decreased gradually with increasing concentration of a specific lectin (from $1 \mu\text{M}$ to $25 \mu\text{M}$ [for details, see Table S1], Fig. 4a–d). Interestingly, the dimeric SPEs 1 (Fig. 4a) and 2 (Fig. 4b) are almost twofold more sensitive than their monomeric counterparts 3 (Fig. 4c) and 4 (Fig. 4d), respectively, which is likely due to the denser sugar clustering at the interface of the former. The limits of detection of 1–4, determined as 16, 25, 88 and 69 nM , respectively ($S/\sigma_b = 3$, where σ_b is the standard deviation of the peak current obtained in the absence of an analyte), also illustrate that the sensitivity of the dimer-confined is better than the monomer-confined SPEs.

To better describe the sugar-lectin interactions at the interfaces, electrochemical impedance spectroscopy (EIS) which is a reliable method for measuring the resistive ability of an interfacial substance was performed using $[\text{Fe}(\text{CN})_6]^{3-/4-}$ as a redox probe (Fig. 4)³³. The

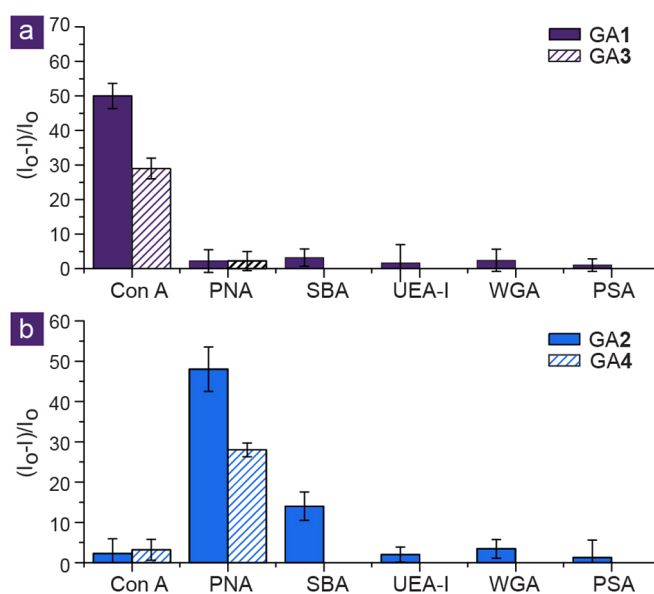


Figure 3 | Differentiation of the specific and non-specific sugar-lectin interactions with the biomimetic interfaces by differential pulse voltammetry (DPV). Current decrease ratio of SPEs confined with (a) GO-GA1 or GO-GA3 and (b) GO-GA2 or GO-GA4 in the presence of various specific and non-specific lectins (where I_0 is the initial current and I is the decreased current) in Tris-HCl (pH 7.0). For the original DPV plots, see Fig. S6 and Fig. S7.

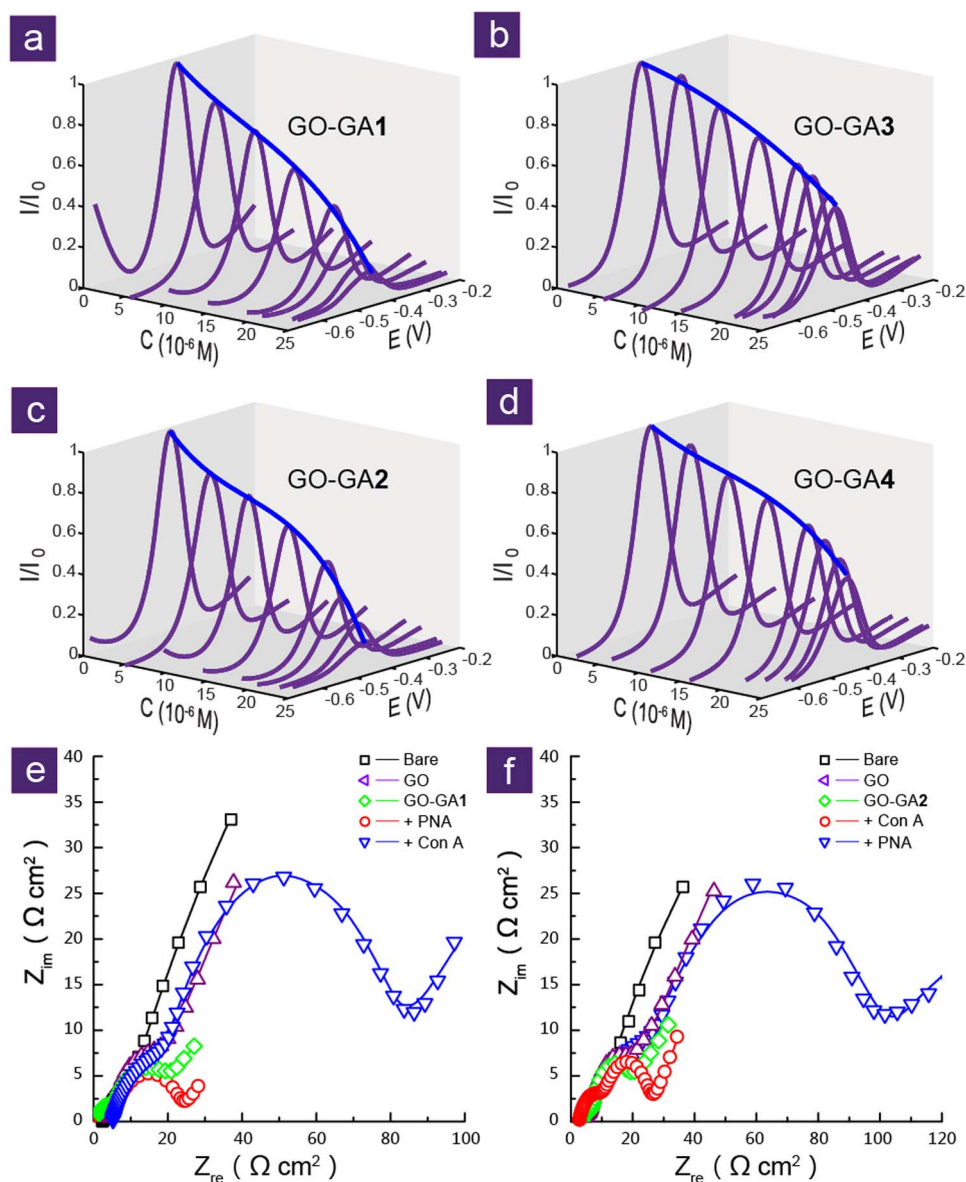


Figure 4 | Probing the specific sugar-lectin interactions with the biomimetic interfaces by DPV and/or electrochemical impedance spectroscopy (EIS). DPVs of SPEs confined with (a) GO-GA1, (b) GO-GA3, (c) GO-GA2 and (d) GO-GA4 in the absence (the top curves) and presence of incremental specific lectins (where I is the changed current after addition of the lectin and I_0 the initial current). For detailed titration data, see Table S1. Experimental (hollow plots) and fitted (lines) Nyquist plots of SPEs in the absence (bare) and presence of (e) GO, GO-GA1, GO-GA1+PNA, and GO-GA1+Con A; (f) GO, GO-GA2, GO-GA2+PNA and GO-GA2+Con A. For circuit models used to fit these Nyquist plots, see Fig. S8. All experiments were performed in Tris-HCl (pH 7.0).

Nyquist plots for bare electrodes exhibited an irregular semicircle at higher frequencies indicating minor electron transfer resistance (R_{et}) and a straight line at lower frequencies that represents the ET process limited by diffusion. While GO was spotted to the electrode surface, additional semicircles indicative of electrochemical reactions between the electrode and a GO-film were recorded. Deposition of GO-GAs 1 and 2 to the electrodes led to further enlarged capacitive loops due to the formation of compound films at the interface. In particular, incubation of Con A with 1 and PNA with 2 (15 μ M) similarly resulted in a much more increased loop, which means that an additional lectin film was probably established at the interface by binding to the densely exposed sugar cluster, causing a greater R_{et} . Addition of a non-specific lectin to the SPE (i.e. PNA to 1 and Con A to 2) led to, however, insignificant R_{et} increment. These data imply that the quenched peak current of the SPEs acquired by DPV is

plausibly caused by “encapsulation” of the glycosyl quinones by lectin³⁴ leading to impaired ET.

Eventually, the ability of the interfacial system to probe sugar-based ligand-receptor interactions was examined with a human hepatocellular carcinoma cell line (Hep-G2) expressing galactose-selective asialoglycoprotein receptors (ASGP-R)³⁵. Incubation of Hep-G2 cells with the galactose-confined SPE 2 led to gradually quenched peak currents (Fig. 5a), implying that the ET process of the galactosyl quinones might be blocked by cells adsorbed at the interface. To verify whether the current decay was caused by cell adsorption as mediated by the specific galactose-ASGP-R recognition, knockdown of ASGP-R1 of Hep-G2 was carried out by RNA interference.

The knockdown assay was performed by transfecting the cells with an ASGP-R1-specific siRNA oligonucleotide duplex or a scrambled

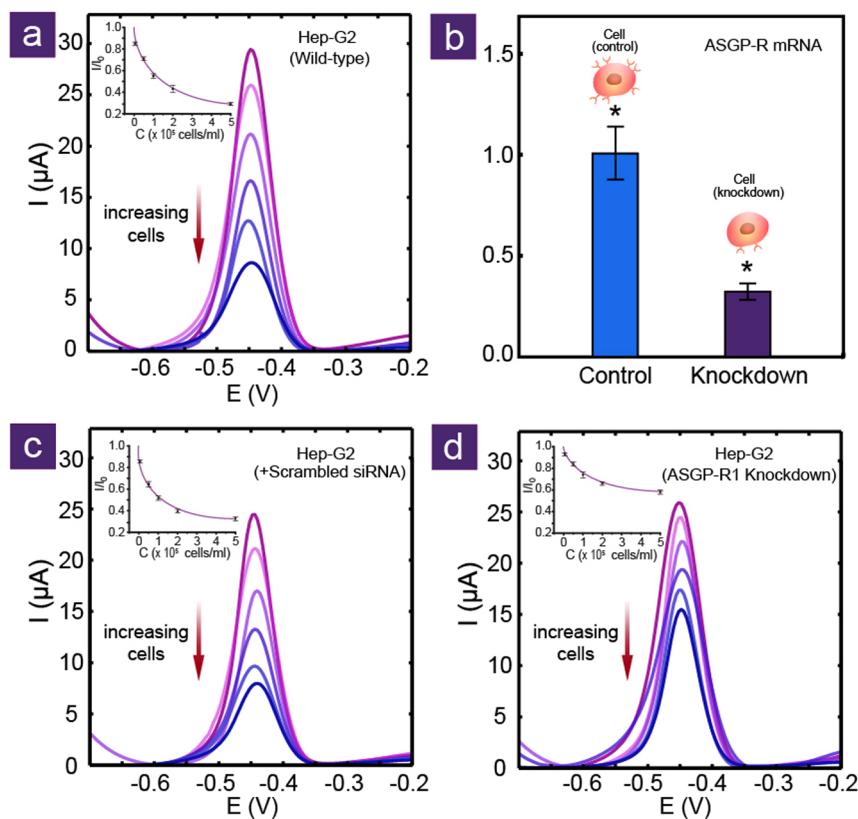


Figure 5 | Probing the sugar-based ligand-receptor interactions with a biomimetic interface by DPV. DPVs of SPEs confined with GO-GA2 in the absence (top curves) and presence of incremental (a) wild-type Hep-G2 cells, (c) control Hep-G2 cells and (d) si-ASGP-R1/Hep-G2 cells (Insets: current decrease ratio, where I_0 is the initial current and I the decreased current in the presence of, from top to bottom, 5,000, 10,000, 100,000, 200,000 and 500,000 Hep-G2 cells/mL). (b) Expression level of ASGP-R1 mRNA of Hep-G2 cells in the presence of a scrambled (control) or a gene-specific siRNA (knockdown) evaluated by quantitative real-time polymerase chain reaction (* $P < 0.003$).

siRNA that does not cause gene silencing as control. Quantitative real-time polymerase chain reaction (RT-PCR) of ASGP-R mRNA indicated that transient transfection of Hep-G2 cells with ASGP-R1-targeting siRNA duplex reduced its transcription level by 70%, whereas a fully retained gene expression was obtained while scrambled siRNA was incubated with Hep-G2 (Fig. 5b)³⁶.

The modified cells were then added to 2 over the same concentration range as employed above. We observed that the presence of increasing control cells caused a gradual current drop with quenching rates approximately identical to those induced by wild-type Hep-G2 (Fig. 5c). Nevertheless, the current quenching of 2 upon addition of the Hep-G2 cells with decreased ASGP-R1 weakened apparently throughout the same cellular concentrations (Fig. 5d). Furthermore, incubation of wild-type Hep-G2 with excessive free methyl *O*-galactosides prior to addition to the SPE resulted in inhibition of the current quenching (Fig. S9b–e). These data suggest that the receptor-ligand recognition indeed contributes to the specific cell capture of the system. Meanwhile, incubation of the glucose-confined SPE 1 with Hep-G2 cells did not cause any current quenching (Fig. S9a,b), indicating the good biospecificity of the biomimetic interfaces at the cellular level.

Discussion

Unlike conventional glycoarray methods, the technique presented here does not require heavy workload to construct the sensing platform and is free of analyte-labelling, a step that might compromise the bio-specificity. By taking advantage of the unique feature of the prepared GAs bearing an anthraquinone moiety that serves both as an electroactive reporter (to produce a signal) and an aromatic tail

that self-assembles to the surface of GO (to realize sugar clustering that reinforces the binding avidity with proteins), biomimetic interfaces were simply fabricated based on easily made SPEs. These interfacial systems have proven to be suitable for sensitive and selective detection of label-free lectins and, especially, cells expressing a specific glycoprotein receptor employing only an inexpensive and portable electrochemical workstation in connection with a personal laptop.

In summary, we have reported on a new tactic for the generation of biomimetic interfaces densely clustered with sugar ligands capable of sensitively capturing glycoprotein receptors on live cancer cells via electrochemical techniques and with economic facilities. The development of this system simply requires a one-step GO-mediated self-assembly of “electrified” anthraquinonyl glycosides to SPEs. We believe that our system due to its simplicity, effectiveness and, especially, admirable biospecificity will become a promising approach for the elaboration of sugar-based ligand-receptor interactions of biological interest.

Methods

Cyclic voltammetry (CV). CVs were recorded with a computer controlled CHI 1232 electrochemical station (Chenhua Co. Ltd, Shanghai, China) between -0.8 V and 0 V (vs. Ag/AgCl) at scan rates ranging from 0 to 120 mV/s. The electrolyte (PBS, 0.5 M, pH = 7.0) used was degassed with N_2 for 20 min before measurements. Screen-printed electrodes (SPEs) were pretreated in PBS (0.05 M, pH 7.0) containing 0.1 M KCl by applying an anodic potential of 2 V (vs. Ag/AgCl) for 2 s, and were then washed with water three times. The circular area (2 mm in diameter) was used as the working electrode; the reference electrode was printed with 40% AgCl in silver paste, and the auxiliary electrode printed with carbon ink. For functionalization of the SPEs, a drop (3 μ L) of the water solution of GO-GAs was dripped onto the working electrode and then dried under vacuum. The functionalized SPEs were finally immersed into PBS solutions for recording the CVs.



Differential pulse voltammetry (DPV). DPVs were recorded with an amplitude of 0.5 V, a pulse width of 0.05 s, a standing time of 2 s, and a scanning range from -0.7 V to 0.2 V in PBS (0.5 M, pH 7.0) or in Tris-HCl (0.5 M, pH 7.0). For detection of analytes, a drop (3 μ L) of the analyte solution (dissolved in PBS or Tris-HCl) of different concentrations was dripped onto the GO-GA functionalized working electrode area of SPE and incubated for 30 min. Then the electrodes were rinsed with the buffer solution three times, dried at room temperature, and then immersed in degassed buffer for measurement.

Electrochemical impedance spectroscopy (EIS). EIS was performed with a ZAHNER apparatus in the presence of the $[\text{Fe}(\text{CN})_6]^{3-}/[\text{Fe}(\text{CN})_6]^{4-}$ (5 mM) redox couple in 0.1 M KCl solution in the frequency range of 10 mHz to 100000 Hz (perturbation signal: 5 mV). All data collected were fitted with the software ZSimpWin. A solution (3 μ L) of GO or GO-GAs was first dripped onto the working electrode area of SPE, dried under vacuum, and then the Nyquist plots recorded. For detection of the sugar-lectin interactions, a drop (Tris-HCl, 3 μ L) of Con A or PNA solution was dripped onto the GO-GA functionalized electrodes, dried under vacuum, followed by recording of the Nyquist plots.

Cell culture. The Hep-G2 cells were obtained from ATCC (Rockville, MD), which were cultured in a Dulbecco's Modified Eagle's Medium (Invitrogen, Carlsbad, CA, USA) supplemented with a 10% Fetal bovine serum (Gibco, Gland Island, NY, USA) at 37°C in a 5% humidified CO_2 air environment.

Silencing of ASGP-R1 gene by RNA interference. Silencing of the ASGP-R1 gene expression on Hep-G2 cells was mediated by an ASGP-R1 gene-specific or a scrambled (control) siRNA oligonucleotide duplex purchased from Santa Cruz Biotechnologies (Santa Cruz, CA). Briefly, HepG2 cells were seeded at 400,000 cells/well in a 6-well plate, and lipofectamine 2000 (Invitrogen) was used for transfection as instructed by the manufacturer. After incubating the cells with siRNAs for 6 h, the lipofectamine-siRNA-complex containing medium was replaced. After another 48 h, the cells were harvested for experiments and the level of ASGP-R1 mRNA was evaluated by quantitative real-time PCR.

Detection of ASGPR mRNA by quantitative RT-PCR. Total cellular RNAs were extracted from HepG2 cells using TRIzol Reagent (Invitrogen) according to the manufacturer's instructions. mRNA was reversely transcribed using the SuperScript First-Strand Synthesis System (TAKARA). For quantitative PCR reactions, 1 : 10 dilutions of cDNA products were amplified using SYBR Green PCR Master Mix (TAKARA) and analyzed by using ABI Prism 7300 Fast system (Applied Biosystems). All samples were run in triplicate in each experiment. The specificity of detected signals was confirmed by a dissociation curve consisting of a single peak. Values were normalized on the basis of GAPDH mRNA. The forward (fp) and reverse (rp) primers for the reactions were as follows:

ASGP-R1-fp: 5'-CTGGACAATGAGGAGAGTGAC-3'
 ASGP-R1-rp: 5'-TTGAAGCCCGTCTCGTAGTC-3'
 GAPDH-fp: 5'-ATCACTGCCACCCAGAAGAC-3'
 GAPDH-rp: 5'-ATGAGGTCCACCACCCTGTT-3'

- Varki, A. Biological roles of oligosaccharides - all of the theories are correct. *Glycobiology* **3**, 97–130 (1993).
- Bertozzi, C. R. & Kiessling, L. L. Chemical glycobiology. *Science* **291**, 2357–2364 (2001).
- Bucior, I. & Burger, M. M. Carbohydrate-carbohydrate interactions in cell recognition. *Curr. Opin. Struct. Biol.* **14**, 631–637 (2004).
- Seeberger, P. H. A spoonful of sugar. *Nature* **437**, 1239 (2004).
- Ohtsubo, K. & Marth, J. D. Glycosylation in cellular mechanisms of health and disease. *Cell* **126**, 855–867 (2006).
- Hart, G. W., Housley, M. P. & Slawson, C. Cycling of O-linked beta-N-acetylglucosamine on nucleocytoplasmic proteins. *Nature* **446**, 1017–1022 (2007).
- Bishop, J. R., Schuksz, M. & Esko, J. D. Heparan sulphate proteoglycans fine-tune mammalian physiology. *Nature* **446**, 1030–1037 (2007).
- Hart, G. W. & Copeland, R. J. Glycomics hits the big time. *Cell* **143**, 672–676 (2010).
- Bertozzi, C. R. & Sasisekharan, R. Glycomics. In *Essentials of Glycobiology*, 2nd Ed. (Eds: Varki, A., Cummings, R. D., Esko, J. D., Freeze, H. H., Stanley, P., Bertozzi, C. R., Hart, G. W., Etzler, M. E.), Cold Spring Harbor, NY: Cold Spring Harbor Laboratory Press, 2009.
- Liu, F.-T. & Rabinovich, G. A. Galectins as modulators of tumor progression. *Nat. Rev. Cancer* **5**, 29–41 (2005).
- Paulson, J. C., Blixt, O. & Collins, B. E. Sweet spots in functional glycomics. *Nat. Chem. Biol.* **2**, 238–248 (2006).
- Ernst, B. & Magnani, J. L. From carbohydrate leads to glycomimetic drugs. *Nat. Drug Discov.* **8**, 661–667 (2009).
- Houseman, B. T. & Mrksich, M. Carbohydrate arrays for the evaluation of protein binding and enzymatic modification. *Chem. Biol.* **9**, 443–454 (2002).
- Wang, D., Liu, S., Trummer, B. J., Deng, C. & Wang, A. Carbohydrate microarrays for the recognition of cross-reactive molecular markers of microbes and host cells. *Nat. Biotech.* **20**, 275–281 (2002).

- Love, K. R. & Seeberger, P. H. Carbohydrate arrays as tools for glycomics. *Angew. Chem. Int. Ed.* **41**, 3583–3586 (2002).
- Feizi, T., Fazio, F., Chai, W. & Wong, C.-H. Carbohydrate microarrays – a new set of technologies at the frontier of glycomics. *Curr. Opin. Struct. Biol.* **13**, 637–345 (2003).
- Wu, C.-Y. & Wong, C.-H. Chemistry and glycobiology. *Chem. Commun.* **47**, 6201–6207 (2011).
- Rostovtsev, V. V., Green, L. G., Fokin, V. V. & Sharpless, K. B. A stepwise Huisgen cycloaddition process: copper(I)-catalyzed regioselective “ligation” of azides and terminal alkynes. *Angew. Chem. Int. Ed.* **41**, 2596–2599 (2002).
- Tornøe, C. W., Christensen, C. & Meldal, M. Peptidotriazoles on solid phase: [1,2,3]-triazoles by regioselective copper(I)-catalyzed 1,3-dipolar cycloaddition of terminal alkynes to azides. *J. Org. Chem.* **67**, 3057–3064 (2002).
- Zhang, Y.-J., He, X.-P., Hu, M., Li, Z., Shi, X.-X. & Chen, G.-R. Highly optically selective and electrochemically active chemosensor for copper (II) based on triazole-linked glucosyl anthraquinone. *Dyes Pigm.* **88**, 391–395 (2011).
- Novoselov, K. S. *et al.* Electric field effect in atomically thin carbon films. *Science* **306**, 666–669 (2004).
- Geim, A. K. & Novoselov, K. S. The rise of graphene. *Nat. Mater.* **6**, 183–191 (2007).
- Park, S. & Ruoff, R. S. Chemical methods for the production of graphenes. *Nat. Nanotechnol.* **4**, 183–191 (2009).
- Geim, A. K. Graphene: status and prospects. *Science* **324**, 1530–1534 (2009).
- Rao, C. N. R., Sood, A. K., Subrahmanyam, K. S. & Govindaraj, A. Graphene: the new two-dimensional nanomaterial. *Angew. Chem. Int. Ed.* **48**, 7752–7777 (2009).
- Xu, Y. & Shi, G. Assembly of chemically modified graphene: methods and applications. *J. Mater. Chem.* **21**, 3311–3323 (2011).
- Compton, O. C. & Nguyen, S. T. Graphene oxide, highly reduced graphene oxide, and graphene: versatile building blocks for carbon-based materials. *Small* **6**, 711–723 (2010).
- Xu, Y., Bai, H., Lu, G., Li, C. & Shi, G. Flexible graphene films via the filtration of water-soluble noncovalent functionalized graphene sheets. *J. Am. Chem. Soc.* **130**, 5856–5857 (2008).
- Kovtyukhova, N. I. *et al.* Layer-by-layer assembly of ultrathin composite films from micron-sized graphite oxide sheets and polycations. *Chem. Mater.* **11**, 771–778 (1999).
- Song, W., Li, D.-W., Li, Y.-T., Li, Y. & Long, Y.-T. Disposable biosensor based on graphene oxide conjugated with tyrosinase assembled gold nanoparticles. *Biosens. Bioelectron.* **26**, 3181–3186 (2011).
- Costentin, C., Robert, M. & Savéant, J.-M. Update 1 of: Electrochemical approach to the mechanistic study of proton-coupled electron transfer. *Chem. Rev.* **110**, PR1–PR40 (2010).
- Guo, X., Kulkarni, A., Doepke, A., Halsall, H. B., Iyer, S. & Heineman, W. R. Carbohydrate-based label-free detection of *Escherichia coli* ORN 178 using electrochemical impedance spectroscopy. *Anal. Chem.* **84**, 241–246 (2012).
- He, X.-P. *et al.* Epimeric monosaccharide-quinone hybrids on gold electrodes toward the electrochemical probing of specific carbohydrate-protein recognitions. *J. Am. Chem. Soc.* **133**, 3649–3657 (2011).
- Lis, H. & Sharon, N. Lectins: carbohydrate-specific proteins that mediate cellular recognition. *Chem. Rev.* **98**, 637–674 (1998).
- Braun, J. R., Willnow, T. E., Ishibashi, S., Ashwell, G. & Herz, J. The major subunit of the asialoglycoprotein receptor is expressed on the hepatocellular surface in mice lacking the minor receptor subunit. *J. Biol. Chem.* **271**, 21160–21166 (1996).
- Yang, J. *et al.* Antisense oligonucleotides targeted against asialoglycoprotein receptor 1 block human hepatitis B virus replication. *J. Viral Hepatit.* **13**, 158–165 (2006).

Acknowledgments

We thank the 973 Project (2013CB733700), the National Science Fund for Distinguished Young Scholars (21125522, 81125023), the National Natural Science Foundation of China (21176076, 21202045), the National Key Science & Technology Specific Projects (012ZX09301-001-004), the Strategic Priority Research Program of the Chinese Academy of Sciences (XDA01040303), the Key Project of Shanghai Science and Technology Commission (13NM1400900) and the Fundamental Research Funds for the Central Universities (WK1013002).

Author contributions

Y.-T.L., X.-P.H., J.L., T.D.J., G.-R.C. and K.C. discussed and conceived of the idea. Z.L. and S.-S.D. performed the experiments. Z.Y., Z.L., X.-P.H. and S.-S.D. analyzed the data. Z.G., Z.L. and X.-P.H. produced the figures. X.-P.H. and T.D.J. wrote and edited the paper. All authors commented on the paper.

Additional information

Supplementary information accompanies this paper at <http://www.nature.com/scientificreports>

Competing financial interests: The authors declare no competing financial interests.



How to cite this article: Li, Z. *et al.* Capturing intercellular sugar-mediated ligand-receptor recognitions via a simple yet highly biospecific interfacial system. *Sci. Rep.* 3, 2293; DOI:10.1038/srep02293 (2013).



This work is licensed under a Creative Commons Attribution-NonCommercial-NoDerivs 3.0 Unported license. To view a copy of this license, visit <http://creativecommons.org/licenses/by-nc-nd/3.0>